ISSN 1541-308X, Physics of Wave Phenomena, 2024, Vol. 32, No. 3, pp. 232–240. © Allerton Press, Inc., 2024.

OPTICAL METHODS FOR THE STUDY OF AQUEOUS SOLUTIONS

Optical Study of the Influence of the Medium Acidity on the Interaction between Gold Nanoparticles and Bovine Serum Albumin in Aqueous Solution

E. A. Molkova[a], *, V. I. Pustovoi[a], I. V. Baimler[a], A. V. Simakin[a], D. E. Burmistrov[a], I. V. Gorudko[b], and S. V. Gudkov[a]

[a] *Prokhorov General Physics Institute of the Russian Academy of Sciences, Moscow, 119991 Russia*

[b] *Physics Department, Belarusian State University, Minsk, 220030 Belarus*

**e-mail: bronkos627@gmail.com*

Received February 9, 2024; revised March 3, 2024; accepted March 4, 2024

Abstract—The influence of the solution acidity on the interaction between bovine serum albumin (BSA) molecules and gold nanoparticles in solutions has been investigated by absorbance spectroscopy, fluorescence spectroscopy, and dynamic light scattering (DLS). The influence of pH on the processes of aggregation–disaggregation of gold nanoparticles with BSA and without it and on the denaturation of protein solution is demonstrated. It is also shown that BSA molecules can stabilize gold nanoparticles at acidic pH values of 2.0–4.0. The data obtained can be useful for physiologists studying the influence of nanoparticles on different biological media of the body.

Keywords: gold nanoparticles, BSA, pH, absorbance spectroscopy, fluorescence spectroscopy, DLS

DOI: 10.3103/S1541308X24700213

1. INTRODUCTION

Optical methods for studying nanoscale media provide information about the concentration of particles, their sizes, composition, and some other parameters. Especially informative is the study of particles exhibiting plasmon resonance, for example, gold ones. Among various types of gold nanoparticles, spherical ones are most widespread because of the simplicity of their synthesis and their relative stability in aqueous solutions [1]. Gold nanoparticles exhibit plasmon resonance, due to which they are widely applied in various test systems [2]. For example, they are used to detect the SARS-CoV-2 virus [3], cancer biomarkers [4], hepatitis B virus [5], ions of different nature, and simple organic compounds [6]. Silver and copper nanoparticles also have similar properties; however, gold nanoparticles are preferred as biosensors specifically due to their high stability and biocompatibility [7]. In particular, chemically unstable nanoparticles (Fe, Co, Mo, Ni, etc.) may oxidize at room temperature [8, 9] or release metal ions and induce cytotoxicity [10].

Having entered a physiological medium, nanoparticles inevitably interact with its components [11]. The result of this interaction is the formation of a "biomolecular corona" on the nanomaterial (adsorption of proteins mainly occurs) [12, 13]. The protein layer on the surface of a nanoparticle increases its size, thus affecting its properties, including optical characteristics [14–16]. Obviously, cell components interact directly with the protein corona rather than with the true surface of nanomaterial [17]. External factors (ionic strength of solution, pH, redox potential, etc.) may affect the properties of proteins during their interaction with nanoparticles [18, 19].

Serum albumin is one of the main proteins of blood plasma (up to 60% of the total content) [20]. Bovine serum albumin (BSA) and human serum albumin have 75.8% similar amino acid sequence and conformation; the low cost of protein make it an excellent candidate for research [21]. When studying the processes occurring in a colloid of nanoparticles with proteins, the most appropriate analytical methods are optical ones, which make it possible to investigate solutions rapidly and non-invasively, multiply repeating measurements. In this paper, we report the results of studying the interaction of BSA molecules with gold nanoparticles in media with different pH, using such optical methods as absorbance spectroscopy, fluorescence spectroscopy, and dynamic light scattering (DLS).

2. EXPERIMENTAL

2.1. Preparation of BSA Solutions

The experimental objects were colloidal BSA solutions. BSA (PanEko, Russia) was dissolved in deionized water to a final concentration of 1 mg/mL

(10^{16} mL^{-1}). Solutions were prepared using Milli-Q water with a resistivity of 18.2 MΩ cm.

2.2. Measurement of the Hydrodynamic Diameter of Molecules

The hydrodynamic diameter of BSA molecules, gold nanoparticles (AuNPs), and their aggregates was recorded using a Zetasizer ULTRA Red Label light scattering analyzer (Malvern Panalytical Ltd., Malvern, UK). Each sample, 2 mL in volume, was placed in a quartz cell at 25°C. Three measurements were performed in each experiment. The measurement technique was described in detail in [22].

2.3. Measurement of Optical Absorption

The optical absorption of the samples was measured with a Cintra 40 spectrophotometer (GBC Cintra 40, Australia) in quartz cells with an optical path length of 10 mm at a temperature of 25°C. The optical density of the samples was recorded in the range of 200–700 nm with a scan rate of 350 nm/min and a slit width of 1 nm. The measurement technique was described in detail in [23].

2.4. Fluorescence Measurements

The fluorescence of BSA colloidal solutions was measured using a Jasco FP-8300 3D fluorimeter (JASCO Applied Sciences, Victoria, British Columbia, Canada). Experiments were performed in a quartz mirror cell with an optical path length of 10 mm; measurements were repeated three times for each series of solutions. Spectra was recorded at a temperature of 25°C. The excitation wavelength was 280 nm; radiation was recorded in the range of 305–450 nm with a scan rate of 100 nm/min. The measurement technique was described in detail in [24].

2.5. ζ-Potential Measurement

The ζ-potential was measured on a Malvern Zetasizer Ultra instrument (Malvern Panalytical Ltd., Malvern, UK) at 25°C, using the ZS Xplorer software. All measurements were performed in the automatic attenuation and measurement mode (range of cycles from 10 to 100 for each measurement) with an interval of 60 s between repetitions. The balancing time was 60 s. The measurement technique was described in detail in [25].

2.6. pH Measurements

The pH measurements were performed using a Seven Excellence S470 pH-meter (Mettler Toledo, Greisensee, Switzerland) in 5-mL quartz flasks, with constant stirring. The pH of solution was controlled by adding dropwise different amounts of HCl (1/0.1/0.01 M) (to acidify the medium) or NaOH (1/0.1/0.01 M) (to alkalize the medium). The pH was varied with a step of about 0.5–1.0. The measurement technique was described in detail in [26].

2.7. Preparation of Gold Nanoparticles

Gold nanoparticles were obtained by laser ablation using a Nd:YAG laser (90 J/cm^2, wavelength 1064 nm, pulse width 10 ns, repetition frequency 8 kHz) [27]. A bulk target consisting of pure gold (99.999%) was placed on the bottom of an experimental glass cell filled with deionized water. The laser beam was moved over the target surface using a 2M electro-galvanic scanner (Atko, Russia) so as to exclude overlap of each new pulse with the previous one [28]. The nanoparticle morphology was investigated using a Libra 200 FE HR transmission electron microscope (Carl Zeiss, Germany).

3. RESULTS

The shape and size of the AuNPs obtained by laser ablation were investigated by transmission electron microscopy (Fig. 1a). The nanoparticles have a spherical shape and a size of about 8–10 nm. The size distributions of particles and aggregates in liquid were determined by DLS. It was shown that individual gold nanoparticles have an average hydrodynamic diameter of 12 nm; the particle concentration turned out to be 3.5×10^{12} per mL. Aggregates, which are also present in solution, have a hydrodynamic diameter of 80 nm with a concentration of 2.6×10^7 mL^{-1}. The concentration ratio of individual gold particles to aggregates turned out to be $10^5 : 1$. To confirm the morphology of particles in solution, we recorded absorption spectra of gold nanoparticles. Peak absorption of gold nanoparticles is observed at a wavelength of 519 nm, which corresponds to the spectrum of a solution of spherical gold nanoparticles with sizes from 10 to 20 nm. To determine the stability of the colloid, we measured its electrokinetic potential, which turned out to be –28 mV.

The DLS technique was used to investigate the influence of pH on the size distribution of aqueous colloids of BSA and/or gold nanoparticles (Fig. 2a). The particle-size distribution indicates the percentage of particles of a certain size (or in a certain range of sizes). The pH of as-prepared BSA solution was 6.2. In this case, a unimodal distribution with a single maximum, corresponding to the size of individual BSA molecules in an aqueous solution (9 nm), is observed. With an increase in pH to 9.5 the particle size does not change, and the monodispersity of the system is retained. With a decrease in the pH of BSA colloid to 5.5 one can observe an increase in the hydrodynamic diameter of protein molecules to 13 nm and the formation of protein aggregates with sizes from 80 to 150 nm.

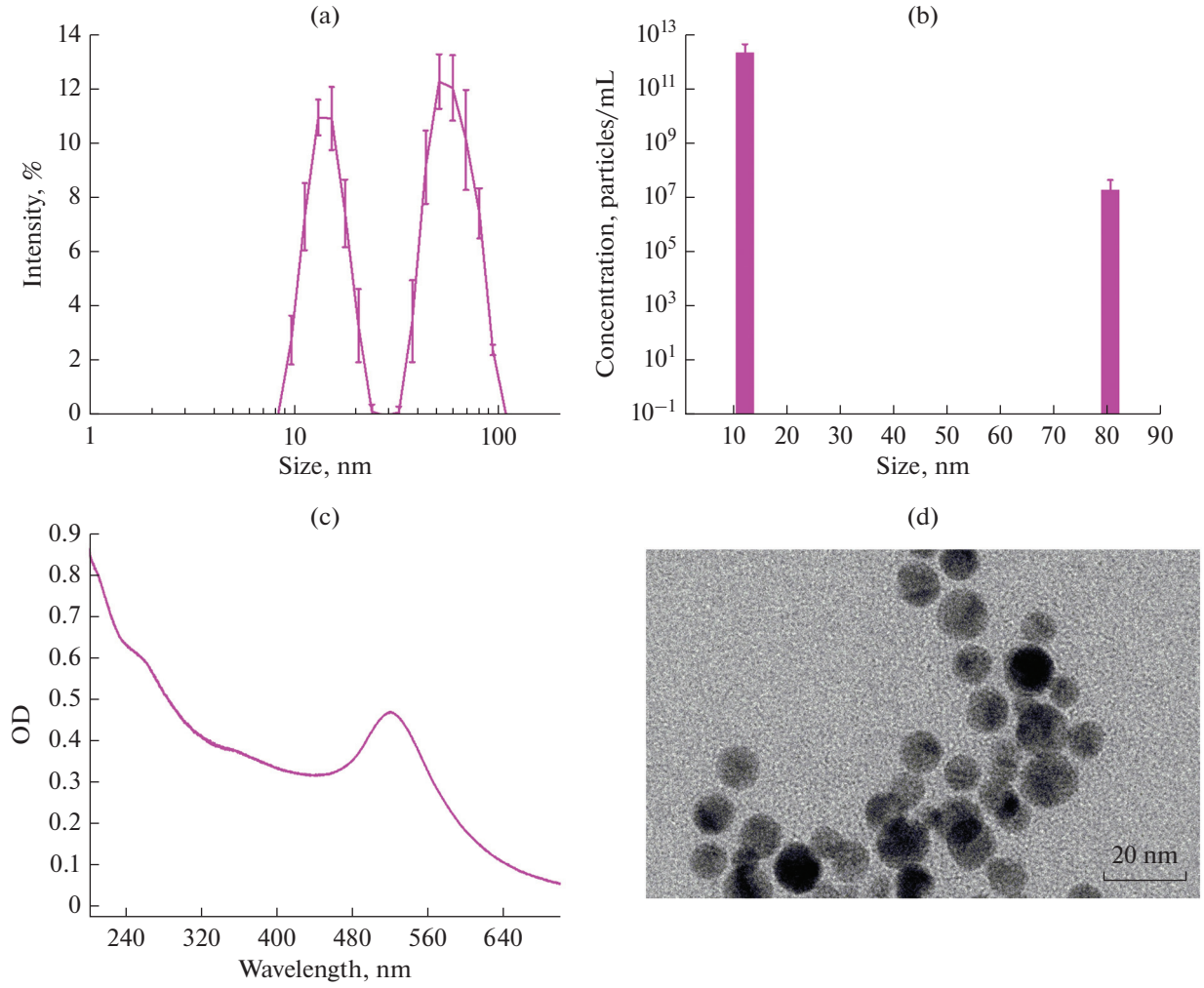

Fig. 1. (Color online) Physical characteristics of a colloidal solution of AuNPs: (a) nanoparticle size distribution in aqueous colloid, (b) concentration of individual nanoparticles and their aggregatesin colloid, (c) absorption spectrum of aqueous colloid of gold nanoparticles, and (d) TEM photograph of gold nanoparticles.

The gold nanoparticles obtained by laser ablation had a concentration of 3.5×10^{12} mL^{-1} and a hydrodynamic diameter of 12 nm; aggregates with sizes of about 80 nm were also present in a small amount (Fig. 2b). The pH of the initial solution was 7.4. With an increase in pH to 10.8 the initial sizes of gold nanoparticles and aggregates slightly increase: up to 25 and 130 nm, respectively. With a decrease in the pH of a solution of freshly prepared nanoparticles to 5.2, a single maximum arises at a size of 90 nm, which corresponds to nanoparticle aggregates. It is noteworthy that with a further decrease in pH the sizes of gold particle aggregates increase to 600 nm, and individual nanoparticles are not observed in the colloid.

The size distribution for a mixture of gold nanoparticles with BSA contains one wide peak with a maximum at 18 nm; the solution pH is 7.1 (Fig. 2c). The separate peak corresponding to single BSA molecules with a maximum at 9 nm is not observed. With an increase in pH to 10.8 the maximum slightly shifts to larger sizes (up to 24 nm). With a decrease in pH of the solution containing protein molecules and gold nanoparticles, beginning with pH 5.2, aggregates with sizes from 70 to 130 nm are formed. With a further decrease in pH to 2.7, the sizes of protein-encapsulated gold nanoparticles and their aggregates increase to 45 and 270 nm, respectively. One wide peak with a maximum of 45 nm is observed at pH 2.0.

In the total size distribution (Fig. 2d) for gold nanoparticles, BSA molecules, and a colloid containing simultaneously gold nanoparticle and BSA molecules, there is a range of pH values from 4.5 to 10.8, in which the sizes of initial gold nanoparticles and protein-encapsulated particles coincide. The aggregates that are present in the initial solution of gold nanoparticles are absent in the colloid containing both BSA molecules and nanoparticles. Likely, addition of protein caused disaggregation of nanoparticles during

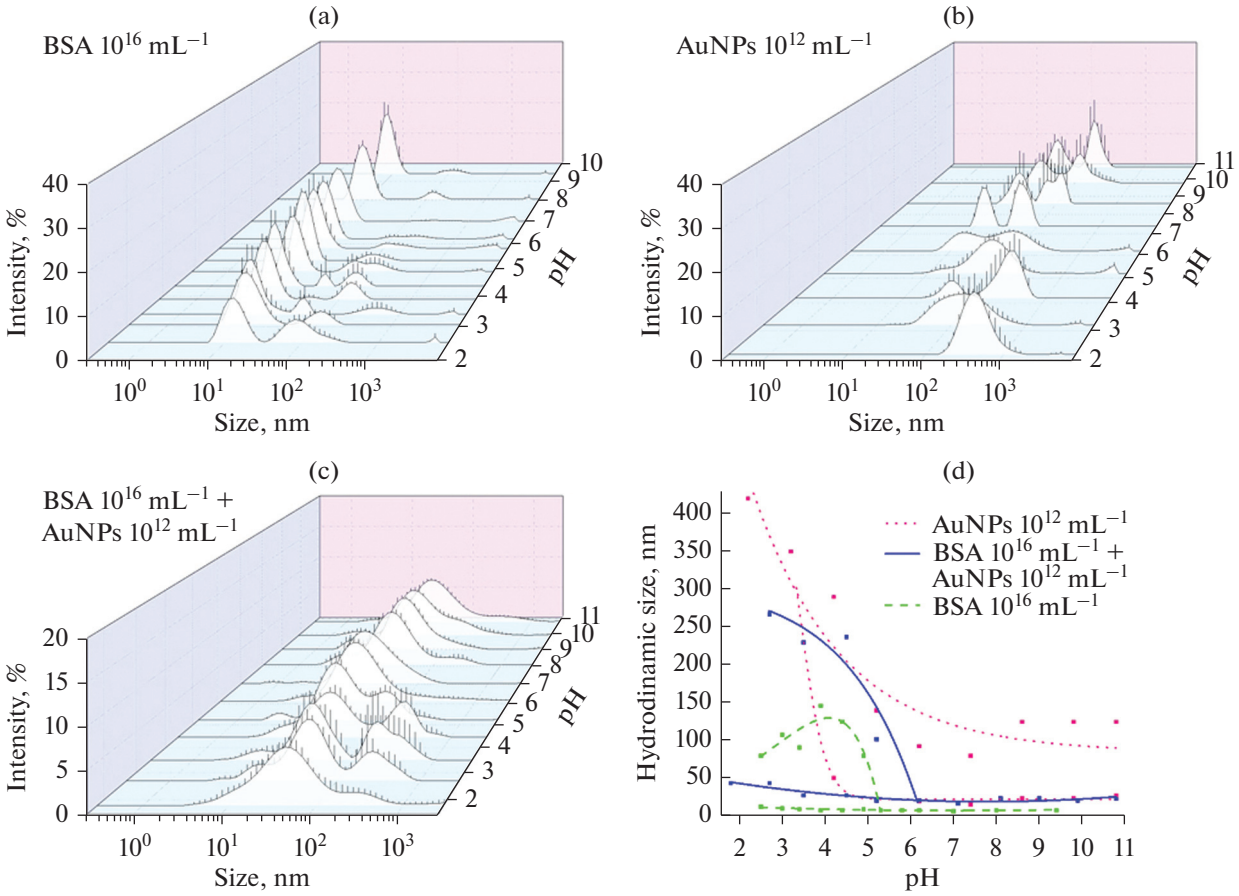

Fig. 2. (Color online) (a–c) Influence of pH on the size distribution of objects in (a) BSA (10^{16} mL^{-1}), (b) AuNPs (10^{12} mL^{-1}), and (c) BSA (10^{16} mL^{-1}) + AuNPs (10^{12} mL^{-1}) colloids. (d) Dependence of the hydrodynamic diameter of objects in BSA (10^{16} mL^{-1}), AuNPs (10^{12}mL^{-1}), and BSA (10^{16} mL^{-1}) + AuNPs (10^{12} mL^{-1}) colloids on pH.

protein adsorption on the nanoparticle surface. However, in the case of BSA (10^{16} mL^{-1}) + AuNPs (10^{12} mL^{-1}) colloid, when adding HCl with pH 6.0, aggregates with sizes from 50 to 270 nm begin to form (upper blue curve). The size of aggregates in the colloidal solution with gold nanoparticles and BSA at pH 5.0 was already 200 nm, which is larger by a factor of 2.5 than that in the initial BSA solution (80 nm aggregates) at the same pH.

The influence of pH on the optical absorption of BSA solutions was investigated (Fig. 3a). It was shown that the maximum absorption of BSA colloid is observed at 277 nm. With a change in the pH, the position of the maximum varies in a narrow range from 275 to 278 nm. The absorption intensity does not change much and varies within 0.58–0.60.

The absorption peak of the solution of gold nanoparticles obtained by laser ablation, with pH 7.4, corresponds to a wavelength 519 nm. It is known that the maximum absorbance depends on the nanoparticle size. The larger the nanoparticle size, the longer the wavelength region the peak shifts to [29]. Significant changes occur when pH decreases to 2.0. The absorption maximum shifts to larger values (up to 580 nm). When adding alkali (KOH) and changing pH to 10.8, the position of the absorption peak for the initial gold solution changes only slightly (to 524 nm). Thus, the DLS data on the size distribution of gold nanoparticles in a wide range of pH are confirmed.

When adding BSA to gold nanoparticles, the position of the absorption peak in the range of the plasmon resonance of gold nanoparticles barely changes with a change in pH. In a wide range of pH, the absorption peaks of the BSA (10^{16} mL^{-1}) + AuNPs (10^{12} mL^{-1}) colloid lie in range of 520–523 nm (Fig. 3c).

The absorption of the BSA initial solution in the entire range of measured pH values changes only slightly (275–278 nm); when adding gold nanoparticles, the positions of the absorption peaks do not change (see Fig. 3c), while the absorption intensity in this range doubles in the colloid with gold nanoparticles. In the range of λ = 510–600 nm the absorption peak position linearly depends on pH.The absorption

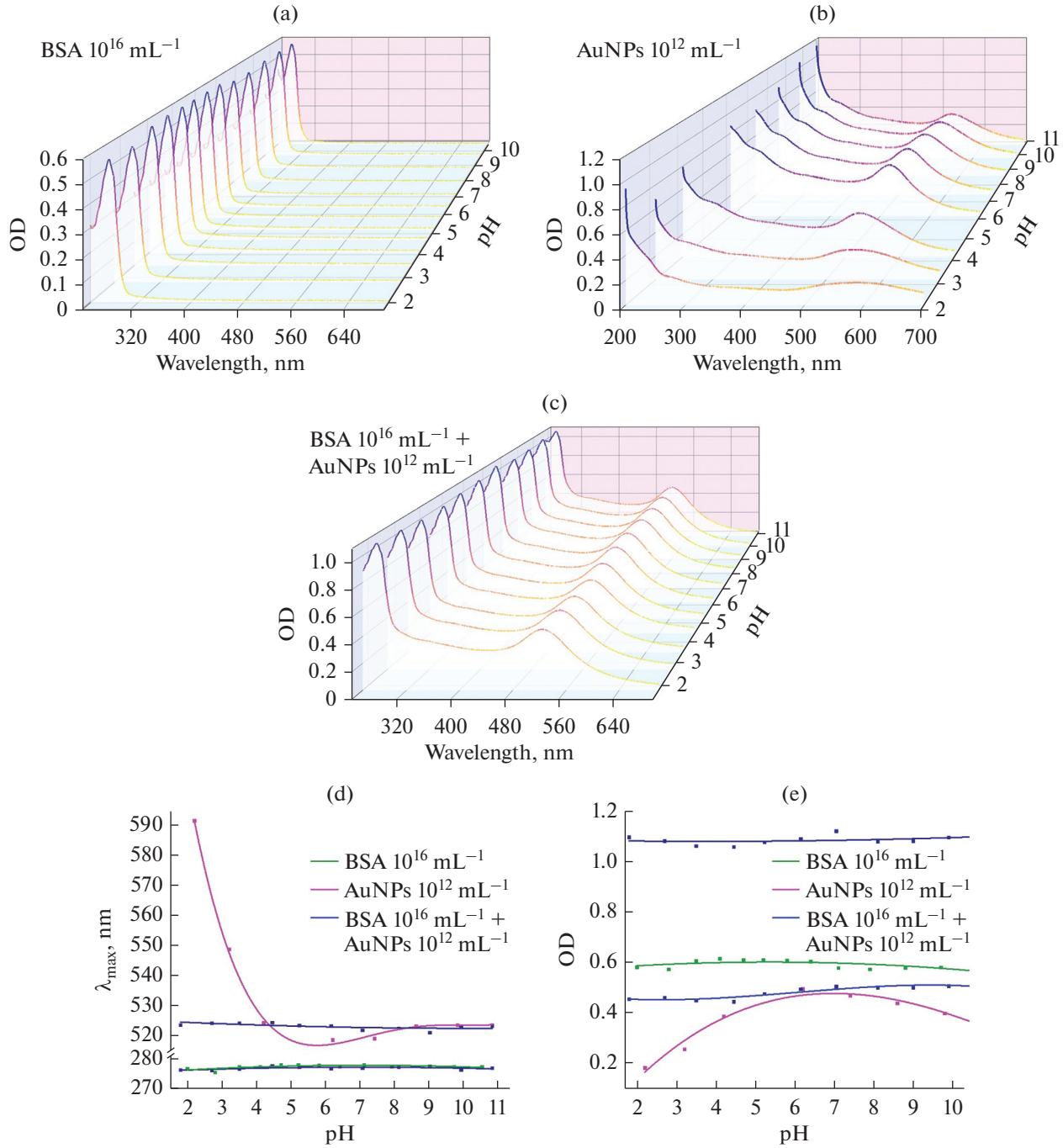

Fig. 3. (Color online) (a–c) Influence of pH on the optical absorption of solutions: (a) BSA (10^{16} mL^{-1}), (b) AuNPs (10^{12} mL^{-1}), and (c) BSA (10^{16} mL^{-1}) + AuNPs (10^{12} mL^{-1}). (d) Dependence of the maximum absorption wavelength λ_{max} on pH for BSA (10^{16} mL^{-1}) + AuNPs (10^{12} mL^{-1}), BSA (10^{16} mL^{-1}), and AuNPs (10^{12} mL^{-1}) colloids.(e) Dependence of the optical density on pH for BSA (10^{16} mL^{-1}) + AuNPs (10^{12} mL^{-1}), BSA (10^{16} mL^{-1}), and AuNPs (10^{12} mL^{-1}) colloids.

intensity also changes only slightly: it increases from 0.44 to 0.50 when pH increases from 2.0 to 10.8.

The dependences of the BSA colloid fluorescence in the presence of gold nanoparticles and without them on the pH of the medium were studied (Fig. 4). The fluorescence of proteins arises due to the presence of certain amino acids in their composition: tyrosine, tryptophan, and phenylalanine. Tryptophan has the highest relative absorbance in comparison with other aromatic amino acids; its absorption peak corresponds to 280 nm. The strongest fluorescence of BSA solution

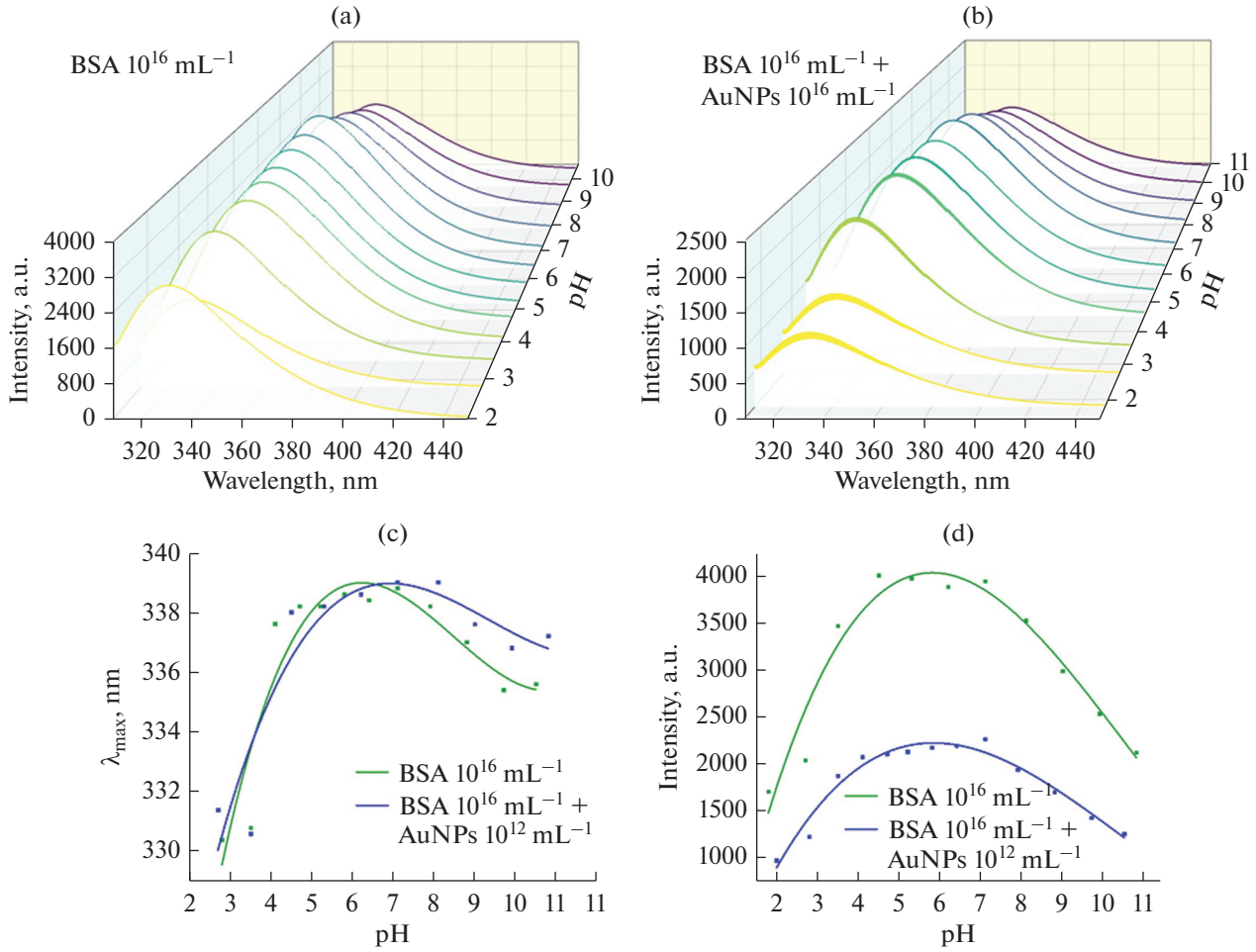

Fig. 4. (Color online) Influence of pH on the fluorescence intensity from (a) BSA (10^{16}mL^{-1}) and (b) BSA (10^{16}mL^{-1}) + AuNPs (10^{12}mL^{-1}) solutions. (c) Dependence of the fluorescence λ_{max} on pH for BSA (10^{16} mL^{-1}) and BSA (10^{16} mL^{-1}) + AuNPs (10^{12} mL^{-1}) colloids. (d) Dependence of the fluorescence intensity on pH for BSA (10^{16} mL^{-1}) and BSA (10^{16} mL^{-1}) + AuNPs (10^{12} mL^{-1}) colloids.

was observed at a wavelength of 339 nm upon excitation at 280 nm. In the range of pH from 4.0 to 7.0 the fluorescence peak lies in the range from 337 to 338 nm. With a decrease in the solution pH to 2.5 the wavelength corresponding to the fluorescence peak (λ_{max}) shifts significantly (to 330 nm), and the fluorescence intensity decreases. An increase in pH causes also a monotonic decrease in the intensity and λ_{max}. Addition of gold nanoparticles to a BSA colloid leads to an increase in λ_{max} by 1 nm for pH ranging from 8.5 to 11.5.

4. DISCUSSION

A change in the acidity of the medium affects the particle size distribution in aqueous solutions of BSA and gold nanoparticles. At pH less than 5.5 molecular aggregates begin to arise in a BSA solution; they increase in size with further decrease in pH (see Fig. 2). This may be related to partial denaturation of protein [30]. With gold nanoparticles added, the aggregation onset shifts by unity to larger values on the pH scale. At pH 2.0–4.0 BSA prevents agglomeration of gold nanoparticles.

The solution of gold nanoparticles with a hydrodynamic diameter of 12 nm, obtained by laser ablation and stable under normal conditions, exhibits maximum absorption at 519 nm. The position of the absorption maximum corresponds to the spectrum of an aqueous colloid of spherical gold nanoparticles whose surface was not subjected to chemical modification [31].

The absorption intensity of BSA colloid in the range of 250–310 nm changes significantly when adding gold nanoparticles. The optical density doubles in comparison with the initial BSA solution. The dependence of the optical density on pH in the range of 450–650 nm for a colloid of gold nanoparticles with

added BSA molecules changes (becomes linear). Addition of BSA to gold nanoparticles, which are unstable in the range of pH from 2.0 to 4.0, prevents their aggregation due to the formation of a "protein corona" on the nanoparticle surface (see Fig. 3). Note that addition of BSA molecules to solutions with pH in the range of 6.0–11.0 does not lead to any significant shift of the maximum absorption wavelength (λ_{max}). The λ_{max} value is determined by the nanoparticle size; an increase in the size of gold spherical nanoparticles causes a red shift of the absorption maximum [32], which confirms reliability of the DLS data for colloids with varied acidity of the medium (see Fig. 2). Specifically, at pH 2.0–4.0 gold nanoparticles form agglomerates with sizes up to several hundreds of nanometers.

The fluorescence of proteins also depends on the acidity of the medium. In the range of pH from 5.0 to 8.0 one can observed maximum fluorescence intensity for pure BSA preparations and BSA with added gold nanoparticles (see Fig. 4). Note that the position of the fluorescence peak changes with a decrease in pH: from 338 nm at pH 4.5 to 330–331 nm at pH 2.5. When the protein denaturates, its fluorescence intensity decreases mainly due to the screening of some amino acid groups of molecules by other groups [33].

5. CONCLUSIONS

Thus, it was established that optical methods can be applied to monitor the change in the state of protein molecules and nanoparticles in aqueous colloids with a change in pH, as well as the interaction of protein molecules with nanoparticles. Changing pH is likely the simplest way to control the protein corona on gold nanoparticles. The data obtained in this study make it possible to monitor the state of colloidal solutions of BSA molecules and AuNPs using one or two simple and available methods. On the whole, BSA molecules can stabilize gold nanoparticles at acidic pH values of 2.0–4.0, which may be useful when studying the influence of nanoparticles on physiological processes. We believe that other important lines of further research may the study of the interaction between proteins and nanoparticles in dependence of the ionic strength [34] and the presence of cosmotropic and chaotropic ions in colloid [35]. The interaction between protein molecules and nanoparticles may be affected by temperature [36], mechanical impacts [37], alternating magnetic fields [38], and hypomagnetic conditions [39].

FUNDING

This work was supported by ongoing institutional funding. No additional grants to carry out or direct this particular research were obtained.

CONFLICT OF INTEREST

The authors of this work declare that they have no conflicts of interest.

REFERENCES

1. L. M. F. Batista, M. Moody, C. Weththasingha, E. Kaplan, I. Faruque, M. S. El-Shall, and K. M. Tibbetts, "Understanding photochemical pathways of laser-induced metal ion reduction through byproduct analysis," *Phys. Chem. Chem. Phys.* **25** (28), 18844–18853 (2023). https://doi.org/10.1039/d3cp00052d
2. B. Khlebtsov, "Functional nanoparticles: Synthesis and practical applications," *Colloid J.* **85** (4), 475–478 (2023). https://doi.org/10.1134/S1061933X2360046X
3. P. Moitra, M. Alafeef, K. Dighe, M. B. Frieman, and D. Pan, "Selective naked-eye detection of SARS-CoV-2 mediated by N gene targeted antisense oligonucleotide capped plasmonic nanoparticles," *ACS Nano* **14** (6), 7617–7627 (2020). https://doi.org/10.1021/acsnano.0c03822
4. I. V. Chernykh, M. A. Kopanitsa, A. V. Shchul'kin, E. N. Yakusheva, A. Yu. Ershov, A. A. Martynenkov, I. V. Lagoda, and A. M. Volkova, "Evaluation of cytotoxicity of gold glyconanoparticles of human colon adenocarcinoma cells," *I. P. Pavlov Russ. Med. Biol. Herald* **31** (2), 255–264 (2023). https://doi.org/10.17816/PAVLOVJ112525
5. X. Wang, Y. Li, H. Wang, Q. Fu, J. Peng, Y. Wang, J. Du, Y. Zhou, and L. Zhan, "Gold nanorod-based localized surface plasmon resonance biosensor for sensitive detection of hepatitis B virus in buffer, blood serum and plasma," *Biosens. Bioelectron.* **26** (2), 404–410 (2010). https://doi.org/10.1016/j.bios.2010.07.121
6. G. Liu, M. Lu, X. Huang, T. Li, and D. Xu, "Application of gold-nanoparticle colorimetric sensing to rapid food safety screening," *Sensors* **18** (12), 4166 (2018). https://doi.org/10.3390/s18124166
7. E. S. Babich, S. Scherbak, D. Kirilenko, V. M. Kondratev, D. Stupin, and A. Lipovskii, "Glasses with biocompatible Au/Ag NPs of governed composition," *J. Phys. D: Appl. Phys.* **57** (13), 135302 (2023). https://doi.org/10.1088/1361-6463/ad12f5
8. H. Chang, B. H. Kim, H. Y. Jeong, J. H. Moon, M. Park, K. Shin, S. I. Chae, J. Lee, T. Kang, B. K. Choi, J. Yang, M. S. Bootharaju, H. Song, S. H. An, K. M. Park, J. Y. Oh, H. Lee, M. S. Kim, J. Park, and T. Hyeon, "Molecular-level understanding of continuous growth from iron-oxo clusters to iron oxide nanoparticles," *J. Am. Chem. Soc.* **141** (17), 7037–7045 (2019). https://doi.org/10.1021/jacs.9b01670
9. I. V. Baimler, A. V. Simakin, V. K. Chevokin, V. A. Podvyaznikov, and S. V. Gudkov, "Features of optical breakdown of aqueous colloidal solutions of ferric oxide (Fe_2O_3) nanoparticles occurring on individual or on two closely located nanoparticles," *Chem. Phys. Lett.* **776**, 138697 (2021). https://doi.org/10.1016/j.cplett.2021.138697

10. A.-L. Bailly, F. Correard, A. Popov, G. Tselikov, F. Chaspoul, R. Appay, A. Al-Kattan, A. V. Kabashin, D. Braguer, and M.-A. Esteve, "*In vivo* evaluation of safety, biodistribution and pharmacokinetics of laser-synthesized gold nanoparticles," *Sci. Rep.* **9** (1), 12890 (2019).
https://doi.org/10.1038/s41598-019-48748-3

11. D. S. Sergeevichev, S. I. Dorovskikh, E. S. Vikulova, E. V. Chepeleva, M. B. Vasiliyeva, T. P. Koretskaya, A. D. Fedorenko, D. A. Nasimov, T. Y. Guselnikova, P. S. Popovetsky, N. B. Morozova, and T. V. Basova, "Vapor-phase-deposited Ag/Ir and Ag/Au film heterostructures for implant materials: Cytotoxic, antibacterial and histological studies," *Int. J. Mol. Sci.* **25** (2), 1100 (2024).
https://doi.org/10.3390/ijms25021100

12. R. Cai and C. Chen, "The crown and the scepter: Roles of the protein corona in nanomedicine," *Adv. Mater.* **31** (45), 1805740 (2019).
https://doi.org/10.1002/adma.201805740

13. T. I. Shabatina, O. I. Vernaya, and M. Y. Melnikov, "Hybrid nanosystems of antibiotics with metal nanoparticles—novel antibacterial agents," *Molecules* **28** (4), 1603 (2023).
https://doi.org/10.3390/molecules28041603

14. Y. Hou, S. Tu, X. Zhao, G. Li, N. Li, and A. Zou, "An integrative method for evaluating the biological effects of nanoparticle-protein corona," *Biochim. Biophys. Acta* **1867** (3), 130300 (2023).
https://doi.org/10.1016/j.bbagen.2022.130300

15. F. E. Galdino, A. S. Picco, L. B. Capeletti, J. Bettini, and M. B. Cardoso, "Inside the protein corona: From binding parameters to unstained hard and soft coronas visualization," *Nano Lett.* **21** (19), 8250–8257 (2021).
https://doi.org/10.1021/acs.nanolett.1c02416

16. E. A. Molkova, V. I. Pustovoy, E. V. Stepanova, I. V. Gorudko, M. E. Astashev, A. V. Simakin, R. M. Sarimov, and S. V. Gudkov, "pH-Dependent HEWL-AuNPs interactions: Optical study," *Molecules* **29** (1), 82 (2023).
https://doi.org/10.3390/molecules29010082

17. H. Yang, C. Hao, Z. Nan, and R. Sun, "Bovine hemoglobin adsorption onto modified silica nanoparticles: Multi-spectroscopic measurements based on kinetics and protein conformation," *Int. J. Biol. Macromol.* **155**, 208–215 (2020).
https://doi.org/10.1016/j.ijbiomac.2020.03.211

18. A. V. Bychkova, M. V. Lopukhova, L. A. Wasserman, Ye. N. Degtyarev, A. L. Kovarski, S. Chakraborti, and V. A. Mitkevich, "The influence of pH and ionic strength on the interactions between human serum albumin and magnetic iron oxide nanoparticles," *Int. J. Biol. Macromol.* **194**, 654–665 (2022).
https://doi.org/10.1016/j.ijbiomac.2021.11.110

19. X. Wang, S. Zhang, Y. Xu, X. Zhao, and X. Guo, "Ionic strength-responsive binding between nanoparticles and proteins," *Langmuir* **34** (28), 8264–8273 (2018).
https://doi.org/10.1021/acs.langmuir.8b00944

20. S. Al-Harthi, J. I. Lachowicz, M. E. Nowakowski, M. Jaremko, and Ł. Jaremko, "Towards the functional high-resolution coordination chemistry of blood plasma human serum albumin," *J. Inorg. Biochem.* **198**, 110716 (2019).
https://doi.org/10.1016/j.jinorgbio.2019.110716

21. A. A. Ksenofontov, P. S. Bocharov, K. V. Ksenofontova, and E. V. Antina, "Water-soluble BODIPY-based fluorescent probe for BSA and HSA detection," *J. Mol. Liq.* **345**, 117031 (2022).
https://doi.org/10.1016/j.molliq.2021.117031

22. R. M. Sarimov, E. I. Nagaev, T. A. Matveyeva, V. N. Binhi, D. E. Burmistrov, D. A. Serov, M. E. Astashev, A. V. Simakin, O. V. Uvarov, V. V. Khabatova, A. G. Akopdzhanov, N. L. Schimanowskii, and S. V. Gudkov, "Investigation of aggregation and disaggregation of self-assembling nano-sized clusters consisting of individual iron oxide nanoparticles upon interaction with HEWL protein molecules," *Nanomaterials* **12** (22), 3960 (2022).
https://doi.org/10.3390/nano12223960

23. E. I. Nagaev, I. V. Baimler, A. S. Baryshev, M. E. Astashev, and S. V. Gudkov, "Effect of laser-induced optical breakdown on the structure of BSA molecules in aqueous solutions: An optical study," *Molecules* **27** (19), 6752 (2022).
https://doi.org/10.3390/molecules27196752

24. S. V. Gudkov, A. V. Simakin, N. F. Bunkin, G. A. Shafeev, M. E. Astashev, A. P. Glinushkin, M. A. Grinberg, and V. A. Vodeneev, "Development and application of photoconversion fluoropolymer films for greenhouses located at high or polar latitudes," *J. Photochem. Photobiol., B* **213**, 112056 (2020).
https://doi.org/10.1016/j.jphotobiol.2020.112056

25. D. E. Burmistrov, A. V. Simakin, V. V. Smirnova, O. V. Uvarov, P. I. Ivashkin, R. N. Kucherov, V. E. Ivanov, V. I. Bruskov, M. A. Sevostyanov, A. S. Baikin, V. A. Kozlov, M. B. Rebezov, A. A. Semenova, A. B. Lisitsyn, M. V. Vedunova, and S. V. Gudkov, "Bacteriostatic and cytotoxic properties of composite material based on ZnO nanoparticles in PLGA obtained by low temperature method," *Polymers* **14** (1), 49 (2022).
https://doi.org/10.3390/polym14010049

26. I. A. Shcherbakov, I. V. Baimler, S. V. Gudkov, G. A. Lyakhov, G. N. Mikhailova, V. I. Pustovoy, R. M. Sarimov, A. V. Simakin, and A. V. Troitsky, "Influence of a constant magnetic field on some properties of water solutions," *Dokl. Phys.* **65** (8), 273–275 (2020).
https://doi.org/10.1134/S1028335820080078

27. A. V. Simakin, I. V. Baimler, V. V. Smirnova, O. V. Uvarov, V. A. Kozlov, and S. V. Gudkov, "Evolution of the size distribution of gold nanoparticles under laser irradiation," *Phys. Wave Phenom.* **29** (2), 102–107 (2021).
https://doi.org/10.3103/S1541308X21020126

28. S. V. Gudkov, M. E. Astashev, I. V. Baimler, O. V. Uvarov, V. V. Voronov, and A. V. Simakin, "Laser-induced optical breakdown of an aqueous colloidal solution containing terbium nanoparticles: the effect of oxidation of nanoparticles," *J. Phys. Chem. B* **126** (30), 5678–5688 (2022).
https://doi.org/10.1021/acs.jpcb.2c02089

29. Y. Q. He, S. P. Liu, L. Kong, and Z. F. Liu, "A study on the sizes and concentrations of gold nanoparticles by spectra of absorption, resonance Rayleigh scattering and resonance non-linear scattering," *Spectrochim. Ac-*

ta, Part A **61** (13–14), 2861–2866 (2005). https://doi.org/10.1016/j.saa.2004.10.035

30. N. Varga, V. Hornok, D. Sebők, and I. Dékány, "Comprehensive study on the structure of the BSA from extended-to aged form in wide (2–12) pH range," *Int. J. Biol. Macromol.* **88**, 51–58 (2016). https://doi.org/10.1016/j.ijbiomac.2016.03.030
31. D. V. Havaldar, R. V. Patil, D. N. Moholkar, P. S. Magdum, A. P. Vadrale, and K. D. Pawar, "Differently synthesized gold nanoparticles respond differently to functionalization with L-amino acids," *Particuology* **52**, 97–104 (2020). https://doi.org/10.1016/j.partic.2019.12.010
32. I. Hammami, N. M. Alabdallah, A. Aljomaa, and M. Kamoun, "Gold nanoparticles: Synthesis properties and applications," *J. King Saud Univ.–Sci.* **33** (7), 101560 (2021). https://doi.org/10.1016/j.jksus.2021.101560
33. S. Barik, A. Mahapatra, N. Preeyanka, and M. Sarkar, "Assessing the impact of choline chloride and benzyltrimethylammonium chloride-based deep eutectic solvents on the structure and conformational dynamics of bovine serum albumin: A combined steady-state, time-resolved fluorescence and fluorescence correlation spectroscopic study," *Phys. Chem. Chem. Phys.* **25** (29), 20093–20108 (2023). https://doi.org/10.1039/D3CP01380D
34. C. Cantarutti, Y. Hunashal, C. La Rosa, M. Condorelli, S. Giorgetti, V. Bellotti, F. Fogolari, and G. Esposito, "The corona of protein-gold nanoparticle systems: The role of ionic strength," *Phys. Chem. Chem. Phys.* **24** (3), 1630–1637 (2022). https://doi.org/10.1039/d1cp04574a
35. H. Akhtar, M. Pourmadadi, F. Yazdian, and H. Rashedi, "Kosmotropic and chaotropic effect of biocompatible Fe_3O_4 nanoparticles on egg white lysozyme; the key role of nanoparticle-protein corona formation," *J. Mol. Struct.* **1253**, 132016 (2022). https://doi.org/10.1016/j.molstruc.2021.132016
36. M. Prawatborisut, S. Jiang, J. Oberländer, V. Mailänder, D. Crespy, and K. Landfester, "Modulating protein corona and materials–cell interactions with temperature-responsive materials," *Adv. Funct. Mater.* **32** (2), 2106353 (2022). https://doi.org/10.1002/adfm.202106353
37. I. A. Shcherbakov, "Current trends in the studies of aqueous solutions," *Phys. Wave Phenom.* **30** (3), 129–134 (2022). https://doi.org/10.3103/S1541308X22030104
38. R. M. Sarimov, D. A. Serov, and S. V. Gudkov, "Biological effects of magnetic storms and ELF magnetic fields," *Biology* **12** (12), 1506 (2023). https://doi.org/10.3390/biology12121506
39. R. M. Sarimov, D. A. Serov, and S. V. Gudkov, "Hypomagnetic conditions and their biological action (review)," *Biology* **12** (12), 1513 (2023). https://doi.org/10.3390/biology12121513

Translated by Yu. Sin'kov